Combined DV–Xα and Gas-Phase UV Photoelectron Spectroscopic Investigation of the Electronic Structures of Tetravalent Titanium, Zirconium, Molybdenum, and Thorium 1-Sila-3-metallacyclobutane Metallocene Complexes†

Enrico Cilberto, Santo Di Bella, Antonino Gulino, and Ignazio Fragalá*

Dipartimento di Scienze Chimiche, Università di Catania, 95125 Catania, Italy

Jeffrey L. Petersen*

Department of Chemistry, West Virginia University, Morgantown, West Virginia 26506

Tobin J. Marks*

Department of Chemistry, Northwestern University, Evanston, Illinois 60208-3113

Received March 21, 1991

The electronic structures of the 1-sila-3-metallacyclobutane complexes, $Cp_2M(CH_2SiMe_2CH_2)$, where $Cp = \eta^5$-C_5H_5 and M = Ti, Zr, Mo, Th, have been investigated by a combination of SCF Hartree–Fock–Slater discrete variational Xα calculations and He I, He II UV photoelectron spectroscopy. Photoelectron data are completely consistent with the energy sequences and valence orbital atomic compositions determined by the theoretical calculations. It is found that these "stabilized" metallacyclobutane complexes are best described electronically as heterodinuclear molecules containing bridging μ-CH_2 groups rather than simple strained hydrocarbyl derivatives. The formation of the four-membered ring involves bonding interactions analogous to those found in cyclobutane. The metal–ligand bonding involves stabilizing interactions between higher-lying empty orbitals of the bridging μ-CH_2 groups and appropriate metal orbitals of the metallocene fragment. The resulting higher-lying molecular orbitals representing the M–C bonds have energies modulated by the relative amount of metal participation. More internal metallacycle molecular orbitals also provide a bonding contribution, although to a smaller extent. The population of these orbitals causes a redistribution of electron densities and, in spite of the high formal metal oxidation state (+4), partially restores the d^2 metal configuration. The 2 + 2 reactivity modes in the related metallacyclobutanes can be accounted for by analyzing the evolution of correlated molecular orbitals of $Cp_2Ti(CH_2SiMe_2CH_2)$, $Cp_2TiCH_2CH_2CH_2$, $Cp_2Ti{=}CH_2(C_2H_4)$, and of noninteracting $Cp_2Ti{=}CH_2 + C_2H_4$ molecules. The titanacyclobutane complex, $Cp_2TiCH_2CH_2CH_2$, can be considered as a latent olefin complex even though the metallacyclic structure is thermodynamically favored. Variation in orbital character and decreasing metal–d or –f covalency (with Ti ≥ Zr ≫ Th) of the LUMO in the corresponding 1-sila-3-metallacyclobutanes is closely connected with differences in reactivity.

Introduction

Metallacyclobutanes[1] and related complexes play a key role[2] in several important classes of organometal-assisted or -catalyzed reactions and continue to develop as useful reagents in molecular[3] and macromolecular[4] synthesis. For early-transition-metal metallacyclobutanes (A), reactivity

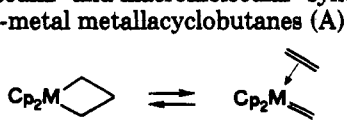

(1)

A

is strongly influenced by both the kinetics and thermodynamics[2c-f,5] of processes which interconvert metallacyclobutanes and the corresponding alkylidene–olefin complexes (e.g., eq 1).[2c,g] While such transformations are widespread in Cp_2Ti chemistry ($Cp = \eta^5$-C_5H_5), their facility decreases markedly as group 4 is descended and are not observed for Cp'_2Th metallacycles ($Cp' = \eta^5$-$(CH_3)_5C_5$).[6] These observations raise general questions about variations in the electronic structures of early-transition-metal and actinide metallacyclobutanes—questions which would be profitably addressed in a correlated photoelectron spectroscopic (PES) experimental–SCF Hartree–Fock discrete variational Xα (DV–Xα) theoretical fashion.

† Abstracted in part from the Ph.D. Thesis of A. Gulino, University of Catania, 1989.

(1) (a) Puddephatt, R. J. *Comments Inorg. Chem.* **1982**, *2*, 69–95 and references therein. (b) Grubbs, R. H. In *Comprehensive Organometallic Chemistry*; Wilkinson, G., Stone, F. G. A., Abel, E. W., Eds.; Pergamon Press: Oxford, U.K., 1982; Vol. 8, Chapter 54, pp 499–551 (see also references therein. (c) Chappell, S. D.; Cole-Hamilton, D. J. *Polyhedron Report Number 2: The Preparation and Properties of Metallacyclic Compounds of the Transition Elements*; Pergamon Press: Oxford, U.K. 1982; Vol. 1, pp 739–777 (see also references therein). (d) Puddephatt, R. J. *Coord. Chem. Rev.* **1980**, *33*, 149–191 and references therein. (e) Al-Essa, R. J.; Puddephatt, R. J.; Quyser, M. A.; Tipper, C. F. H. *J. Am. Chem. Soc.* **1979**, *101*, 364–370. (f) Grubbs, R. H. *Prog. Inorg. Chem.* **1978**, *24*, 1–50 and references therein. (g) Andersen, R. A.; Jones, R. A.; Wilkinson, G. *J. Chem. Soc., Dalton Trans.* **1978**, 446–453. (h) Al-Essa, R. J.; Puddephatt, R. J.; Quyser, M. A.; Tipper, C. F. H. *J. Organomet. Chem.* **1978**, *150*, 295–307.

(2) (a) Erker, G.; Mean, M.; Hoffmann, U.; Menjon, B.; Petersen, J. L. *Organometallics* **1991**, *10*, 291–298. (b) Meinhart, J. D.; Anslyn, E. V.; Grubbs, R. H. *Organometallics* **1989**, *8*, 583–589. (c) Anslyn, E. V.; Santarsiero, B. D.; Grubbs, R. H. *Organometallics* **1988**, *7*, 2137–2145. (d) Anslyn, E. V.; Grubbs, R. H. *J. Am. Chem. Soc.* **1987**, *109*, 4880–4890. (e) Lee, J. B.; Ott, K. C.; Grubbs, R. H. *J. Am. Chem. Soc.* **1982**, *104*, 7491–7496. (f) Strauss, D. A.; Grubbs, R. H. *Organometallics* **1982**, *1*, 1658–1661. (g) Howard, T. R.; Lee, J. B.; Grubbs, R. H. *J. Am. Chem. Soc.* **1980**, *102*, 6876–6878. (h) Tebbe, F. N.; Parshall, G. W.; Ovenall, D. W. *J. Am. Chem. Soc.* **1979**, *101*, 5074–5075. (i) Ivin, K. J.; Rooney, J. J.; Stewart, C. D.; Green, M. L. H.; Magtab, R. *J. Chem. Soc., Chem. Commun.* **1978**, 604–606. (j) Ephritikhine, M.; Francis, B. R.; Green, M. L. H.; Mackenzie, R. E.; Smith, M. J. *J. Chem. Soc., Dalton Trans.* **1977**, 1131–1135.

0276-7333/92/2311-1727$03.00/0

Table I. Orbitals, Eigenvalues, Ionization Energies, and Population Analysis for $Cp_2\overline{Ti(CH_2Si(CH_3)_2CH_2)}$[a]

MO[b]	−eV GS	−eV TSIE	eV IE[c]	Ti 4s	Ti 4p	Ti 3d	2Cp	$2CH_2$	$Si(CH_3)_2$	dominant character
$15a_1$	3.09			0	0	70	10	11	9	d_{z^2} (42%) + $d_{x^2-y^2}$ (28%)
$14a_1$	5.72	8.25	7.41 (a)	1	0	20	4	63	12	$CH_2 + d_{x^2-y^2}$
$12b_1$	6.310	8.74	8.05 (b′)	0	0	11	86	3	0	$\pi_2 + d_{xz}$
$9b_2$	6.314	8.80	8.23 (b)	0	1	32	2	62	3	$CH_2 + d_{yz}$
$7a_2$	6.71	9.07	8.75 (c)	0	0	14	83	3	0	$\pi_2 + d_{xy}$
$8b_2$	6.84	9.18	9.03 (c′)	0	2	0	87	9	2	π_2
$13a_1$	7.14	9.56	9.56 (d)	0	0	8	91	1	0	$\pi_2 + d_{z^2}$
$11b_1$	7.80	10.63	9.98 (e)	0	0	0	0	12	88	Si–CH_3
$7b_2$	7.92	10.94	10.35 (f)	0	0	5	7	60	28	Si–C + d_{yz}
$12a_1$	8.87	11.61	11.24 (g)	0	0	1	4	28	67	Si–C
$10b_1$	9.46			0	0	1	96	3	0	π_1
$11a_1$	10.41			0	0	0	96	2	2	π_1

Overall Charge
Ti = $3d^{1.98}$, $4s^{0.10}$, $4p^{0.10}$ = +1.82
Cp = −0.513
$Si(CH_3)_2$ = +0.628
$-CH_2-$ = −0.713

[a] Corresponding data on empty orbitals are given in Table SI. [b] $15a_1$ = LUMO, $14a_1$ = HOMO. [c] Lettering in parentheses refers to the band labels in Figure 5.

Although experimental analysis of metallacycle electronic structure and the electronic constraints upon eq 1 would be most attractively pursued with simple metallacyclobutanes, most are not of sufficient thermal stability[6,7] for high-quality PES studies. In contrast, closely related 1-sila-3-metallacyclobutanes (B) exhibit considerably enhanced thermal stability and have been chemically/structurally/spectroscopically characterized for a range of early transition metals and Th.[6,8] In this contribution, we present a comparative, combined He I, He II PES–DV–Xα theoretical study of electronic structure in the d^0, d^2, and f^0 silametallacycles $Cp_2\overline{M(CH_2SiMe_2CH_2)}$ (M = Ti, Zr, Mo) and $Cp'_2\overline{Th(CH_2SiMe_2CH_2)}$. We also compare theoretically the electronic structures of $Cp_2\overline{TiCH_2CH_2CH_2}$ and $Cp_2\overline{Ti(CH_2SiMe_2CH_2)}$ as well as examine the electronic structural changes that occur upon traversing the reaction coordinate of eq 1 for $Cp_2\overline{TiCH_2CH_2CH_2}$.

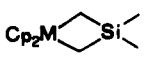

B

Experimental Section

The complexes $Cp_2\overline{M(CH_2SiMe_2CH_2)}$ (M = Ti, Zr, Mo) and $Cp'_2\overline{Th(CH_2SiMe_2CH_2)}$ were prepared in accordance with published procedures[6,8] and purified by vacuum sublimation or recrystallization. High-resolution PE spectra were accumulated with an IBM AT computer directly interfaced to a PE spectrometer equipped with a He I/He II (Helectros Development) source. Resolution measured on the He $1s^{-1}$ line was always ca. 20 meV. The He II spectra were only corrected for the He II β "satellite" contributions (13% on the N_2 reference spectrum).

Computational Details. Quantum mechanical calculations were carried out within the SCF Hartree–Fock–Slater first-principles discrete variational Xα formalism,[9] using previously described procedures to approximate the electron density,[9] to evaluate the coulomb potential,[9] and to converge SCF equations.[9] Such procedures have been shown to give excellent agreement with PES results for a wide range of molecules containing both d and f valence atomic orbitals (AOs).[10] Numerical AOs[9] (through 4p on Ti, 5p on Zr and Mo, 7p on Th, 3d on Si, 2p on C, and 1s on H) were used as basis functions. A frozen core approximation (1s, ..., 3p on Ti; 1s, ..., 4p on Zr and Mo; 1s, ..., 6p on Th; 1s, ..., 2p on Si; 1s on C) was used throughout the calculations.[9] The ionization energies (IEs) were evaluated within the Slater transition-state formalism[11] (TSIEs) to account for reorganization effects upon ionization. Contour plots (CPs) of several selected molecular orbitals (MOs) were also analyzed. Calculations for the Th complex were made for the model $Cp_2\overline{Th(CH_2SiMe_2CH_2)}$ at a nonrelativistic level. Previous work has shown that while neglect of relativistic effects for Th complexes causes an overestimation of 5f versus 6d orbital participation, the MO ordering and derivable chemical information remains largely unchanged.[12]

(3) (a) General reference: Collman, J. P.; Hegedus, L. S.; Norton, J. R.; Finke, R. G. *Principles and Applications of Organotransition Metal Chemistry*; University Science Books: Mill Valley, CA, 1987; pp 459–520. (b) Brown-Wensley, K. A.; Buchwald, S. L.; Cannizzo, L.; Clauson, L.; Ho, S.; Meinhardt, D.; Stille, J. R.; Straus, D.; Grubbs, R. H. *Pure Appl. Chem.* **1983**, *55*, 1733–1744.

(4) (a) Schrock, R. R. *Acc. Chem. Res.* **1990**, *23*, 158–165. (b) Gilliom, L. K.; Grubbs, R. H. *J. Am. Chem. Soc.* **1986**, *108*, 733.

(5) Lee, J. B.; Gajda, G. J.; Schaefer, W. P.; Howard, T. R.; Ikarida, T.; Straus, D. A.; Grubbs, R. H. *J. Am. Chem. Soc.* **1981**, *103*, 7358–7361.

(6) (a) Smith, G. M.; Carpenter, J. D.; Marks, T. J. *J. Am. Chem. Soc.* **1986**, *108*, 6805–6807. (b) Fendrick, C. M.; Marks, T. J. *J. Am. Chem. Soc.* **1986**, *108*, 425–437. (c) Bruno, J. W.; Smith, G. M.; Marks, T. J.; Fair, C. K.; Schultz, A. J.; Williams, J. M. *J. Am. Chem. Soc.* **1986**, *108*, 40–56. (d) Bruno, J. W.; Marks, T. J.; Day, V. W. *J. Am. Chem. Soc.* **1982**, *104*, 7357–7360.

(7) Seetz, J. W. F. L.; Schat, G.; Akkerman, O. S.; Bickelhaupt, F. *Angew. Chem., Int. Ed. Engl.* **1983**, *22*, 248.

(8) (a) Tikkanen, W.; Ziller, J. W. *Organometallics* **1991**, *10*, 2266–2273. (b) Amorose, D. M.; Lee, R. A.; Petersen, J. L. *Organometallics* **1991**, *10*, 2191–2198. (c) Tikkanen, W. R.; Egan, J. W., Jr.; Petersen, J. L. *Organometallics* **1984**, *3*, 1646–1650. (d) Tikkanen, W. R.; Liu, J. Z.; Egan, J. W., Jr.; Petersen, J. L. *Organometallics* **1984**, *3*, 825–830. (e) Petersen, J. L. Unpublished results.

(9) (a) Trogler, W. C.; Ellis, D. E.; Berkowitz, J. *J. Am. Chem. Soc.* **1979**, *101*, 5896–5901. (b) Rosen, A.; Ellis, D. E.; Adachi, H.; Averill, F. W. *J. Chem. Phys.* **1976**, *65*, 3629–3634 and references therein. (c) Averill, F. W.; Ellis, D. E. *J. Chem. Phys.* **1973**, *59*, 6411–6418.

(10) (a) Casarin, M.; Ciliberto, E.; Gulino, A.; Fragalá, I. *Organometallics* **1989**, *8*, 900–906. (b) Bursten, B. E.; Casarin, M.; Ellis, D. E.; Fragalá, I.; Marks, T. J. *Inorg. Chem.* **1986**, *25*, 1257–1261. (c) Vittadini, A.; Casarin, M.; Ajó, D.; Bertoncello, R.; Ciliberto, E.; Gulino, A.; Fragalá, I. *Inorg. Chim. Acta* **1986**, *121*, L23–L25. (d) Ellis, D. E. In *Actinides in Perspective*; Edelstein, N. M., Ed.; Pergamon: Oxford, U.K., 1982; p 123.

(11) Slater, J. C. *Quantum Theory of Molecules and Solids. The Self-Consistent Field for Molecules and Solids*; McGraw-Hill: New York, 1974; Vol. 4.

(12) (a) Pepper, M.; Bursten, B. E. *Chem. Rev.* **1991**, *91*, 719–741. (b) Boerrigter, P. M.; Baerends, E. J.; Snijders, J. G. *Chem. Phys.* **1988**, *122*, 357–374. (c) Boerrigter, P. M.; Snijders, J. G.; Dyke, J. M. *J. Electron Spectrosc. Relat. Phenom.* **1988**, *46*, 43–53. (d) Hohl, D.; Ellis, D. E.; Rösch, N. *Inorg. Chim. Acta* **1987**, *127*, 195–202. (e) Rösch, N. *Inorg. Chim. Acta* **1984**, *94*, 297–299.

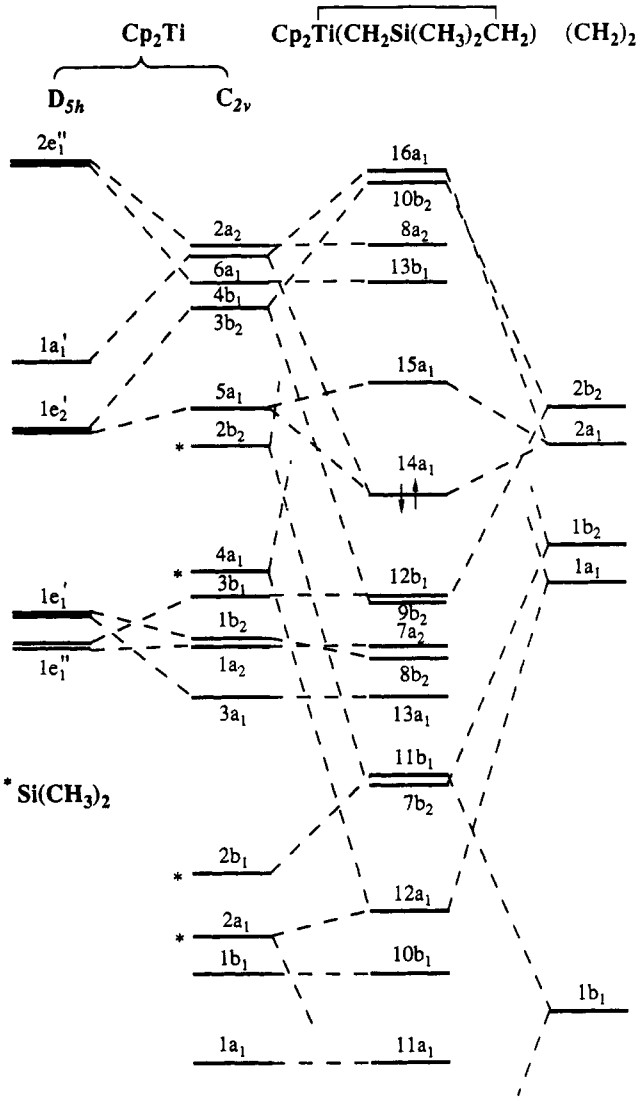

Figure 1. Formation diagram for the $Cp_2\overline{Ti(CH_2SiMe_2CH_2)}$ molecule involving ground-state eigenvalues of the Cp_2Ti, $SiMe_2$, and $(CH_2)_2$ fragments. The energy scale from $14a_1$ through $15a_1$ MOs is compressed by a factor of 2.

Geometrical parameters used for calculations on $Cp_2\overline{M(CH_2SiMe_2CH_2)}$ (M = Ti, Zr, Mo, Th), $Cp_2\overline{TiCH_2CH_2CH_2}$, $Cp_2Ti{=}CH_2(C_2H_4)$, and $Cp_2Ti{=}CH_2$ were taken from published data or reasonable estimations.[6c,8,13] All of the calculations were performed on a VAX-11/750 minicomputer.

Results

Electronic Structures of $Cp_2\overline{M(CH_2SiMe_2CH_2)}$ Complexes (M = Ti, Zr, Mo, Th). Computational Results. Theoretical ground-state (GS) and transition-state (TSIE), as well as experimental, ionization energies associated with filled MOs of $Cp_2\overline{Ti(CH_2SiMe_2CH_2)}$, are summarized in Table I. The outermost occupied MOs are arranged in an expected energy sequene on the basis of their dominant atomic contributions. Within the context of a simple localized bonding model,[14] the filled $14a_1$ (HOMO) and the $9b_2$ orbitals correspond to the symmetry combinations of the two Ti–C σ bonds. In marked contrast to results obtained for several related $(cyclopentadienyl)_2M(CH_3)_2$ complexes,[15] as well as to the MO ordering found in a similar Xα–DV calculation for $Cp_2Zr(CH_3)_2$,[15e] the $14a_1$ in-phase linear combination appears less tightly bound than the out-of-phase combination $9b_2$. The $12b_1$ and the nest of $7a_2$, $8b_2$, and $13a_1$ MOs represent the set of Cp π_2-related[15,16] orbitals and contain considerably less 3d metal character than the $14a_1$ and $9b_2$ orbitals involved in Ti–C σ bonding. The remaining orbitals fall in two general categories with $11b_1$, $7b_2$, and $12a_1$ representing the Si–C interactions within the metallacyclic ring and the Si–C(methyl)bonds and $10b_1$ and $11a_1$ being associated with internal Cp ring π electrons.

These findings are a suitable basis for a qualitative electronic structure description using a localized bond interaction scheme. However, any simple description of the electronic structure of $Cp_2\overline{Ti(CH_2SiMe_2CH_2)}$ as a classical $Cp_2M(hydrocarbyl)_2$ complex[15] is unable to account for the $14a_1$ MO lying above the $9b_2$. An alternative description that considers $Cp_2\overline{Ti(CH_2SiMe_2CH_2)}$ as a heterodinuclear bis(μ-methylene) species[17] offers a considerably more attractive representation of the principal features of the electronic structure.

The electronic structure of a closed-shell Cp_2M fragment[18] (C_{2v} symmetry) and the orbitals generated upon canting the rings from a metallocene sandwich configuration are well understood.[10a,19] Bending causes a splitting of metal-based orbitals (Figure 1). The new orbitals $5a_1$ and $3b_2$ (from $1e_2'$) and $6a_1$ (from $1a_1'$) are destabilized, reflecting greater σ-antibonding character, mixing with other available orbitals of a_1 symmetry, and better overlap with the metal d_{z^2} orbital ($5a_1$). The concommitant stabilization of the $4b_1$ and $2a_2$ orbitals (from $2e_1''$), due to weaker antibonding interactions, ultimately produces a narrower range of metal orbital energies for the bent C_{2v} than for the D_{5h} metallocene structure. With the relatively small ring centroid–M–ring centroid angles found in Cp_2MX_2 complexes,[8,20] the energy of the $4b_1$ metal-based orbital is displaced below that of the $6a_1$ orbital (Figure 1), thereby inverting the energy ordering normally encountered.[10a,19] Opposite effects are observed for filled π_2-related MOs upon bending. The $1b_2$ and $3a_1$ MOs (derived from e_1') are stabilized (Figure 1) because of interactions, now allowed by symmetry, with d orbitals.[21]

(13) Upton, T. H.; Rappé, A. K. *J. Am. Chem. Soc.* **1985**, *107*, 1206–1218.
(14) Evans, S.; Hamnett, A.; Orchard, A. F.; Lloyd, D. R. *Faraday Discuss. Chem. Soc.* **1972**, *54*, 227–250.
(15) (a) Ciliberto, E.; Condorelli, G.; Fagan, P. J.; Manriquez, J. M.; Marks, T. J. *J. Am. Chem. Soc.* **1981**, *103*, 4755–4759. (b) Creber, D. K.; Bancroft, G. M. *Inorg. Chem.* **1980**, *19*, 643–648. (c) Cowley, A. H. *Prog. Inorg. Chem.* **1979**, *26*, 45–145. (d) Green, J. G.; Jackson, S. E. *J. Chem. Soc., Dalton Trans.* **1976**, 1698–1702. (e) Gulino, A.; Fragalá, I. Unpublished results.
(16) (a) Evans, S.; Green, M. L. H.; Jewitt, A. F.; King, G. H.; Orchard, A. F. *J. Chem. Soc., Faraday Trans. 2* **1974**, *70*, 356–376. (b) Evans, S.; Green, M. L. H.; Jewitt, A. F.; Orchard, A. F.; Pygall, C. F. *J. Chem. Soc., Faraday Trans. 2* **1972**, *68*, 1847–1865.
(17) (a) Mackenzie, P. B.; Coots, R. J.; Grubbs, R. H. *Organometallics* **1989**, *8*, 8–14. (b) Bursten, B. E.; Cayton, R. H. *J. Am. Chem. Soc.* **1986**, *108*, 8241–8249. (c) Jemmis, E. D.; Pinhas, A. R.; Hoffmann, R. *J. Am. Chem. Soc.* **1980**, *102*, 2576–2585. (d) Benard, M. *Inorg. Chem.* **1979**, *18*, 2782–2785.
(18) Wailes, P. C.; Coutts, R. S. P.; Weigold, H. *Organometallic Chemistry of Titanium, Zirconium, and Hafnium*; Academic: New York, 1974; p 229.
(19) Lauher, J. W.; Hoffmann, R. *J. Am. Chem. Soc.* **1976**, *98*, 1729–1742.
(20) (a) Schock, L. E.; Brock, C. P.; Marks, T. J. *Organometallics* **1987**, *6*, 232–241 and references therein. (b) Atwood, J. L.; Rogers, R. D.; Hunter, W. E.; Floriani, C.; Fachinetti, G.; Chiesi-Villa, A. *Inorg. Chem.* **1980**, *19*, 3812–3817.
(21) Note that $1b_2$ and $3a_1$ relate to the D_{5h} e_1' orbitals which, by symmetry, mix with the d subshells.

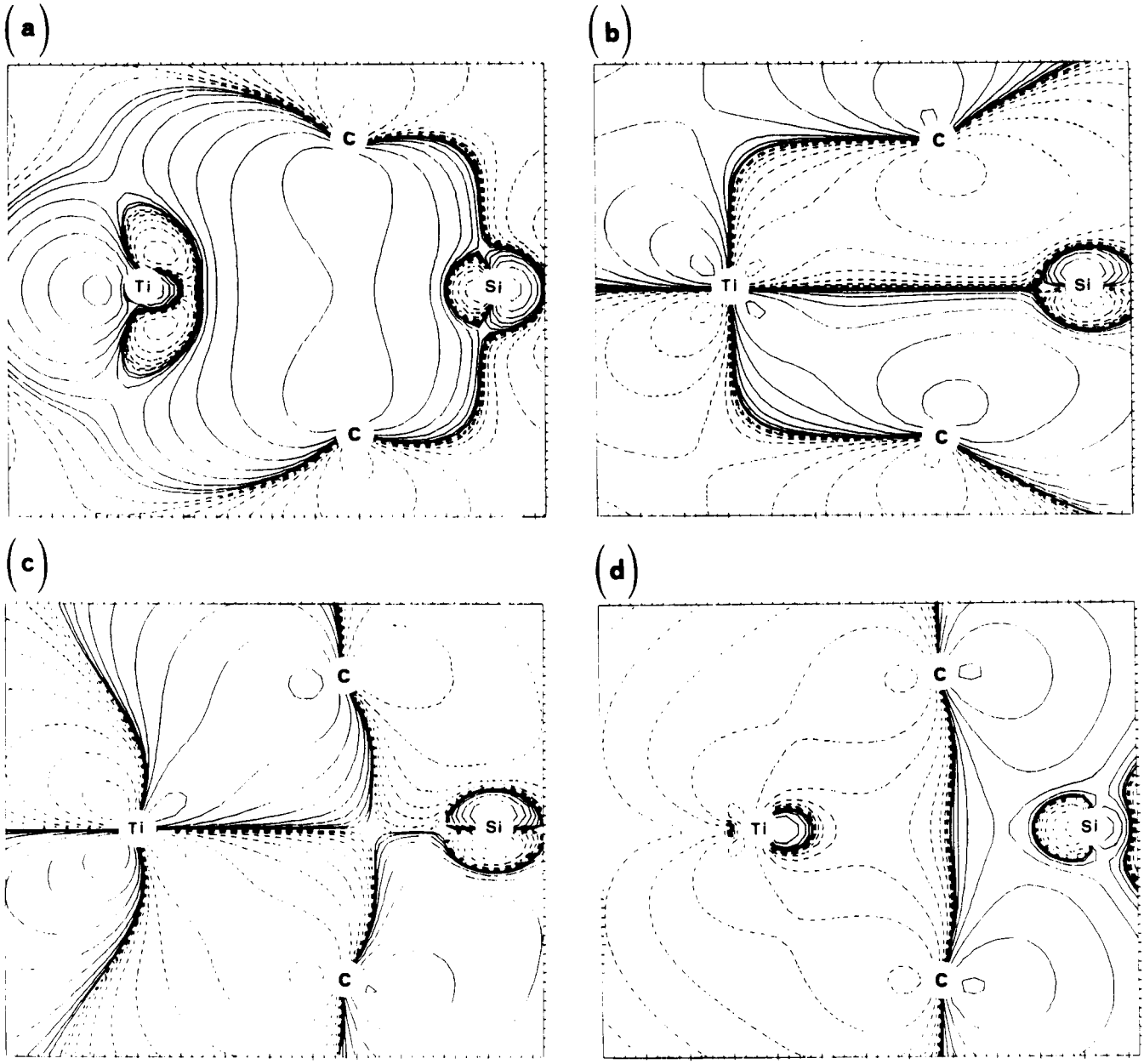

Figure 2. DV-Xα contour plots for the (a) $12a_1$, (b) $7b_2$, (c) $9b_2$, and (d) $14a_1$ MOs of the $Cp_2\overline{Ti(CH_2SiMe_2CH_2)}$ molecule in the *yz* plane. The contour values are ±0.0065, ±0.013, ±0.026, ±0.052, ±0.104, ±0.208, ±0.416, and ±0.832 $e^{1/2}$ Å$^{3/2}$. Dashed lines refer to negative values.

The $3b_1$ and $1a_2$ orbitals suffer a sizeable destabilization because the greater interligand repulsion upon bending outweighs improved overlap with metal-d orbitals.[19]

Each bridging methylene group can be considered as a classical C_{2v}, six-electron, AB_2 system[22] with the relevant MOs being similar to those of H_2O. Among the three filled MOs, two represent C–H σ bonds while the lower-lying one formally represents a C_{2p} lone pair. Alternatively, the electronic structure of this fragment closely resembles that of the π-acid CO ligand, exhibiting both donor and acceptor properties.[17b] The corresponding σ lone pair ($1a_1$) lies in the metallacyclic ring plane and topologically resembles the 5σ CO orbital. The empty 2p methylene carbon orbital ($2b_2$) also lies in the MC_2 plane and corresponds to the analogous CO $2\pi^*\|$MO.[17b] Simple Hückel considerations indicate that these two orbitals in the bridging methylene group are closer to their energy baricenter than in CO. Thus, the methylene ligand acts as a better π-acceptor and σ-donor than CO.[17b] The general features and sequence of relevant MOs of the $>SiMe_2$ fragment are similar,[23] but the larger differences in their relative energies[23] make the fragment a strong σ-donor only.

The electronic structure of the present 1-sila-3-titanacyclobutane metallocene complex can now be formulated by considering the interaction between the relevant orbitals of the Cp_2Ti moiety, the two CH_2, and the $SiMe_2$ fragments (Figure 1). Bridging of the Cp_2Ti and $SiMe_2$ units involves, despite the greater mixing allowed by the lower C_{2v} symmetry, considerably different sets of $(\mu\text{-}CH_2)_2$

(22) (a) Albright, T. A.; Burdett, J. K.; Whangbo, M. H. *Orbital Interactions in Chemistry*; Wiley: New York, 1985; pp 39–42. (b) Williams, A. F. *A Theoretical Approach to Inorganic Chemistry*; Springer-Verlag: Berlin, 1979; p 66.

(23) (a) Dyke, J. M.; Josland, G. D.; Lewis, R. A.; Morris, A. *J. Phys. Chem.* **1982**, *86*, 2913–2916. (b) Koenig, T.; McKenna, W. *J. Am. Chem. Soc.* **1981**, *103*, 1212–1213. (c) Cundy, C. S.; Lappert, M. F.; Pedley, J. B.; Schmidt, W.; Wilkins, B. T. *J. Organomet. Chem.* **1973**, *51*, 99–104.

Table II. Orbitals, Eigenvalues, Ionization Energies, and Population Analysis for $Cp_2\overline{Zr(CH_2Si(CH_3)_2CH_2)}$[a]

MO[b]	−eV GS	−eV TSIE	eV IE[c]	Zr 5s	Zr 5p	Zr 4d	2Cp	$2CH_2$	$Si(CH_3)_2$	dominant character
$15a_1$	2.94			0	1	60	20	11	8	d_{z^2} (33%) + $d_{x^2-y^2}$ (27%) + π_3
$14a_1$	5.80	8.39	7.52 (a)	3	1	16	3	67	10	$CH_2 + d_{x^2-y^2}$
$9b_2$	6.41	8.86	8.29 (b′)	0	2	19	15	62	2	$CH_2 + d_{yz}$
$12b_1$	6.56	8.97	8.52 (b)	0	0	9	88	3	0	$\pi_2 + d_{xz}$
$8b_2$	6.99	9.27	9.08 (c)	0	0	7	80	9	4	$\pi_2 + d_{yz}$
$7a_2$	7.17	9.55	9.21 (c′)	0	0	12	85	3	0	$\pi_2 + d_{xy}$
$13a_1$	7.19	9.57	9.72 (d)	0	1	7	90	1	1	$\pi_2 + d_{z^2}$
$7b_2$	8.04	10.76	10.08 (e)	0	0	6	7	61	26	Si–C + d_{yz}
$11b_1$	7.87	10.93	10.32 (f)	0	0	0	2	7	91	$Si–CH_3$
$12a_1$	8.99	11.55	11.19 (g)	0	0	3	6	27	64	Si–C
$10b_1$	9.64	12.02		0	0	2	97	1	0	π_1
$11a_1$	10.36			0	0	0	99	1	0	π_1

Overall Charge
Zr = $4d^{1.91}$, $5s^{0.129}$, $5p^{0.105}$ = +1.85
Cp = −0.534
$Si(CH_3)_2$ = +0.524
$-CH_2-$ = −0.653

[a] Corresponding data on empty orbitals are given in Table SII. [b] $15a_1$ = LUMO, $14a_1$ = HOMO. [c] Lettering in parentheses refers to the band labels in Figure 6.

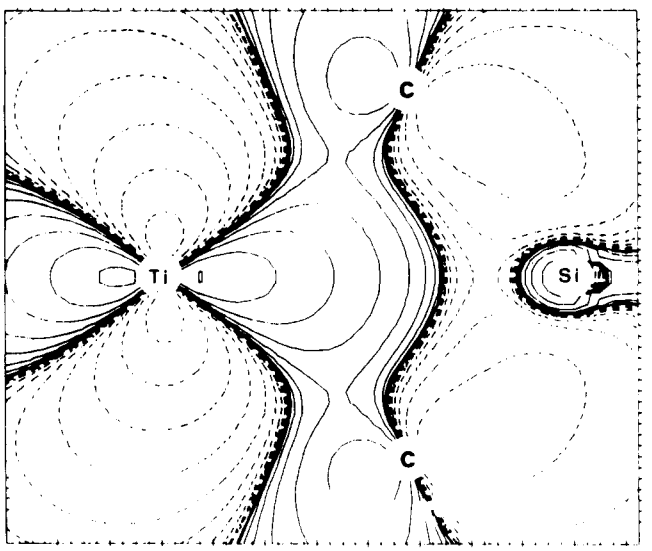

Figure 3. DV-Xα contour plot for the $15a_1$ MO of the $Cp_2\overline{Ti(CH_2SiMe_2CH_2)}$ molecule in the *yz* plane. The contour values are ±0.0065, ±0.013, ±0.026, ±0.052, ±0.104, ±0.208, ±0.416, and ±0.832 $e^{1/2}$ Å$^{3/2}$. Dashed lines refer to negative values.

cluster orbitals (Table I, Figure 1). Bridging of the $>SiMe_2$ group basically involves a *four-orbital–six-electron* interaction between *filled* methylene "lone pair" orbitals ($1a_1$, $1b_2$) and the $>SiMe_2$ orbitals of appropriate symmetry (*filled* $4a_1$ and *empty* $2b_2$). This interaction produces two low-lying bonding MOs ($12a_1$ and $7b_2$) and two high-energy orbitals (off the scale in Figure 1). The bridging of the bent titanocene involves empty orbitals in a *four-orbital–zero-electron* interaction between the methylene $2a_1$ and $2b_2$ and the Cp_2Ti $3b_2$ and $6a_1$ orbitals. This interaction lowers the energies of the $14a_1$ and $9b_2$ MOs in the complex, which are now occupied by an electron pair formerly associated with the $(\mu\text{-}CH_2)_2SiMe_2$ system and by an electron pair formally Cp_2Ti in character. The unexpected energy ordering (i.e., $14a_1 > 9b_2$) is a consequence of the greater admixture of 3d metal character (32%) in the $9b_2$ MO than in $14a_1$ MO (Table I). The corresponding electron density contour diagrams for the occupied $12a_1$, $7b_2$, $9b_2$, and $14a_1$ MOs of the Ti complex are illustrated in Figure 2. It is noteworthy that they are isolobal counterparts of the uppermost filled MOs of cyclobutane[24] and that they provide

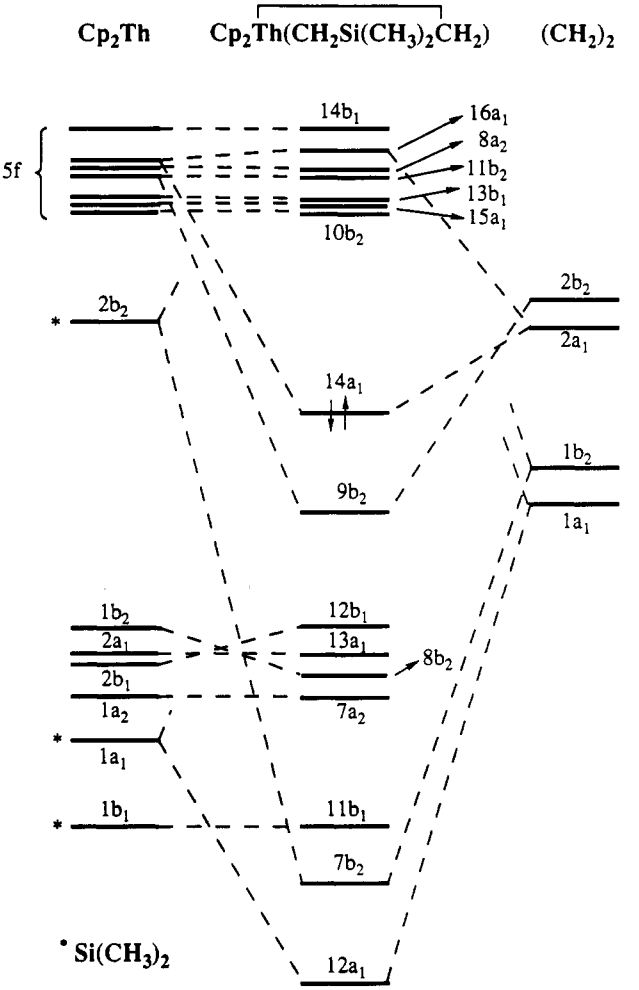

Figure 4. Approximate formation diagram for the $Cp_2\overline{Th(CH_2SiMe_2CH_2)}$ molecule involving ground-state eigenvalues of the Cp_2Th, $SiMe_2$, and $(CH_2)_2$ fragments.

a clear indication that more favorable overlap between interacting fragment orbitals is primarily responsible for

(24) (a) Chu, S. Y.; Hoffmann, R. *J. Chem. Phys.* **1982**, *86*, 1289–1297. (b) Hoffmann, R.; Davison, R. B. *J. Am. Chem. Soc.* **1971**, *93*, 5699–5705. (c) The calculated S_{ij} overlap integral values are 0.1327 for Ti d_{yz}–C_{pz} ($9b_2$) and 0.1052 for Ti $d_{x^2-y^2}$–C_{pz} ($14a_1$).

Table III. Orbitals, Eigenvalues, Ionization Energies, and Population Analysis for $Cp_2\overline{Mo(CH_2Si(CH_3)_2CH_2)}$[a]

MO[b]	−eV GS	−eV TSIE	eV IE[c]	Mo 5s	Mo 5p	Mo 4d	2Cp	$2CH_2$	$Si(CH_3)_2$	dominant character
$13b_1$	1.83			0	0	46	52	2	0	$d_{xz} + \pi_2 + \pi_3$
$15a_1$	4.14	6.75	5.98 (x)	0	0	65	17	11	7	$d_{x^2-y^2} \approx d_{z^2}$
$14a_1$	5.77	8.32	7.57 (a)	3	0	22	6	59	10	$CH_2 + d_{x^2-y^2}$
$9b_2$	6.15	8.69	7.97 (b)	0	2	31	44	23	0	$CH_2 + d_{yz} + \pi_2$
$8b_2$	7.12	9.52		0	0	5	39	29	27	Si–C + π_2
$12b_1$	7.15	9.62	8.86 (c)	0	0	15	81	4	0	$\pi_2 + d_{xz}$
$7b_2$	7.64	10.01	9.53 (d)	0	0	9	81	4	6	$\pi_2 + d_{yz}$
$7a_2$	7.74	10.21	9.94 (e)	0	0	19	78	3	0	$\pi_2 + d_{xy}$
$13a_1$	7.86	10.25		0	1	9	88	2	0	$\pi_2 + d_{z^2}$
$11b_1$	7.40	10.52	10.31 (f)	0	0	0	1	5	94	Si–CH_3
$12a_1$	8.51	11.09	10.87 (g)	0	0	4	3	32	61	Si–C
$10b_1$	10.12	12.58		0	0	3	90	4	3	π_1
$11a_1$	11.05			0	0	0	99	1	0	π_1

Overall Charge
Mo = $4d^{4.409}$, $5s^{0.105}$, $5p^{0.074}$ = +1.413
Cp = −0.417
$Si(CH_3)_2$ = +0.546
$-CH_2-$ = −0.5625

[a] Corresponding data on empty orbitals are given in Table SIII. [b] $13b_1$ = LUMO, $15a_1$ = HOMO. [c] Lettering in parentheses refers to the band labels in Figure 7.

Table IV. Orbitals, Eigenvalues, Ionization Energies, and Population Analysis for $Cp_2\overline{Th(CH_2Si(CH_3)_2CH_2)}$[a]

MO[b]	−eV GS	−eV TSIE	eV IE[c]	Th 7s	Th 7p	Th 6d	Th 5f	2Cp	$2CH_2$	$Si(CH_3)_2$	dominant character
$10b_2$	3.88			0	0	11	84	4	1	0	$f_{yz^2} + d_{yz}$
$14a_1$	4.95	7.28	6.83 (a)	1	0	3	15	13	64	4	$CH_2 + f_{z(x^2-y^2)}$
$9b_2$	5.57	7.71	7.09 (b)	0	0	7	9	35	47	2	$CH_2 + f_{yz^2}$
$12b_1$	6.17	8.29		0	0	4	4	77	12	3	π_2
$13a_1$	6.29	8.33	7.43 (c′)	0	0	5	6	89	0	0	π_2
$8b_2$	6.40	8.35	7.62 (c)	0	0	9	4	64	20	3	$\pi_2 + d_{yz}$
$7a_2$	6.54	8.51	7.93 (d)	0	0	8	3	89	0	0	$\pi_2 + d_{xy}$
$11b_1$	7.24	9.95	8.91 (e)	0	0	2	2	1	58	37	Si–C
$7b_2$	7.54	10.20	9.19 (f)	0	0	0	0	0	4	96	Si–CH_3
$12a_1$	8.04	10.59	9.50 (g)	0	0	3	0	1	21	75	Si–C
$10b_1$	9.27			0	0	1	0	99	0	0	π_1
$6a_2$	9.42			0	0	0	0	0	2	98	σ

Overall Charge
Th = $5f^{0.87}$, $6d^{0.87}$, $7s^{0.03}$, $7p^{0.05}$ = +2.18
Cp = −0.655
$Si(CH_3)_2$ = +0.56
$-CH_2-$ = −0.715

[a] Corresponding data on empty orbitals are given in Table SIV. [b] $10b_2$ = LUMO $14a_1$ HOMO. [c] Lettering in parentheses refers to the band labels in Figure 8.

Table V. Orbitals, Eigenvalues, and Population Analysis for $Cp_2Ti{=}CH_2(C_2H_4)$

MO[a]	−eV GS	Ti 4s	Ti 4p	Ti 3d	2Cp	CH_2	C_2H_4	dominant character
21a′	1.95	3	1	16	11	30	39	$\pi(C_2H_4) + CH_2 + d_{x^2-y^2}$
20a′	5.19	0	2	34	13	42	9	$CH_2 + d_{z^2}$
16a″	6.05	0	0	10	80	10	0	$\pi_2 + d_{xy}$
15a″	6.43	0	0	11	89	0	0	$\pi_2 + d_{yz}$
19a′	6.49	0	0	7	86	5	2	π_2
18a′	7.08	0	0	13	81	6	0	$\pi_2 + d_{z^2} + d_{x^2-y^2}$
17a′	7.18	0	0	20	12	65	3	$CH_2 + d_{xz}$
16a′	8.28	0	0	1	12	2	85	$\pi(C_2H_4)$
7a′	15.81	0	0	0	9	0	91	$\sigma(C_2H_4)$

Overall Charge
Ti = $3d^{2.09}$, $4s^{0.047}$, $4p^{0.12}$ = +1.74
Cp = −0.571
C_2H_4 = −0.102
$=CH_2$ = −0.496

[a] 21a′ = LUMO, 20a′ = HOMO.

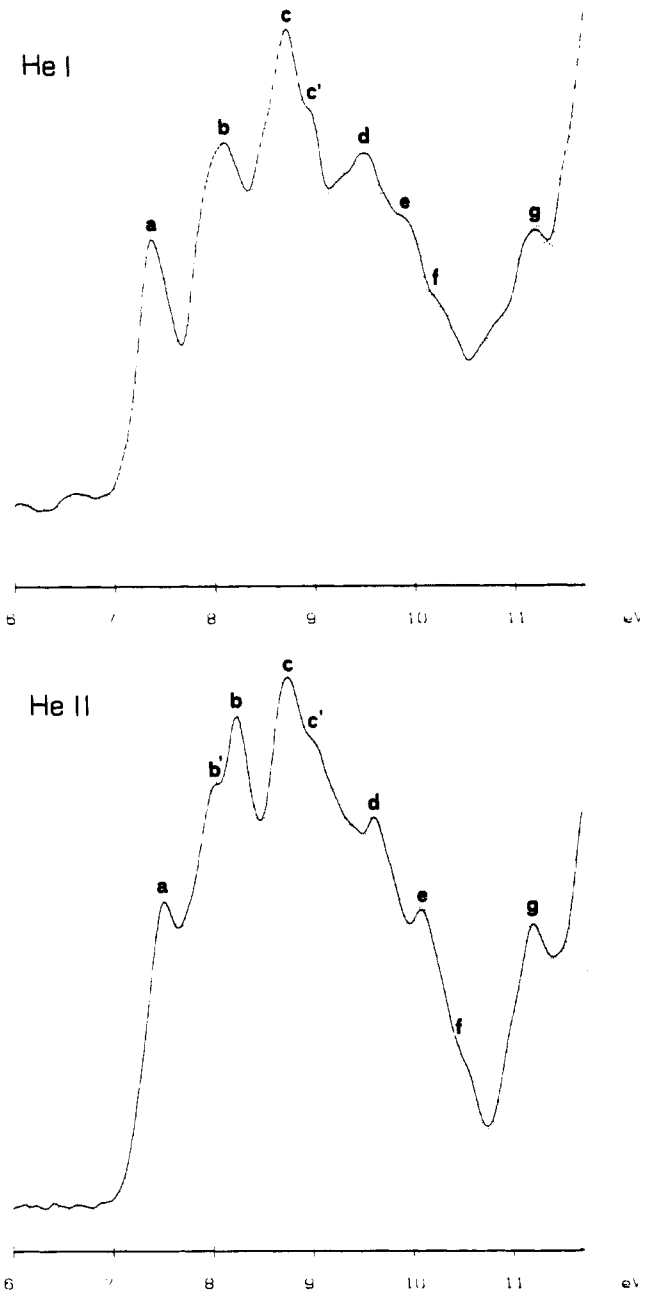

Figure 5. He I and He II photoelectron spectra of $Cp_2\overline{Ti}$-$(CH_2SiMe_2CH_2)$ (6.0–11.8-eV region).

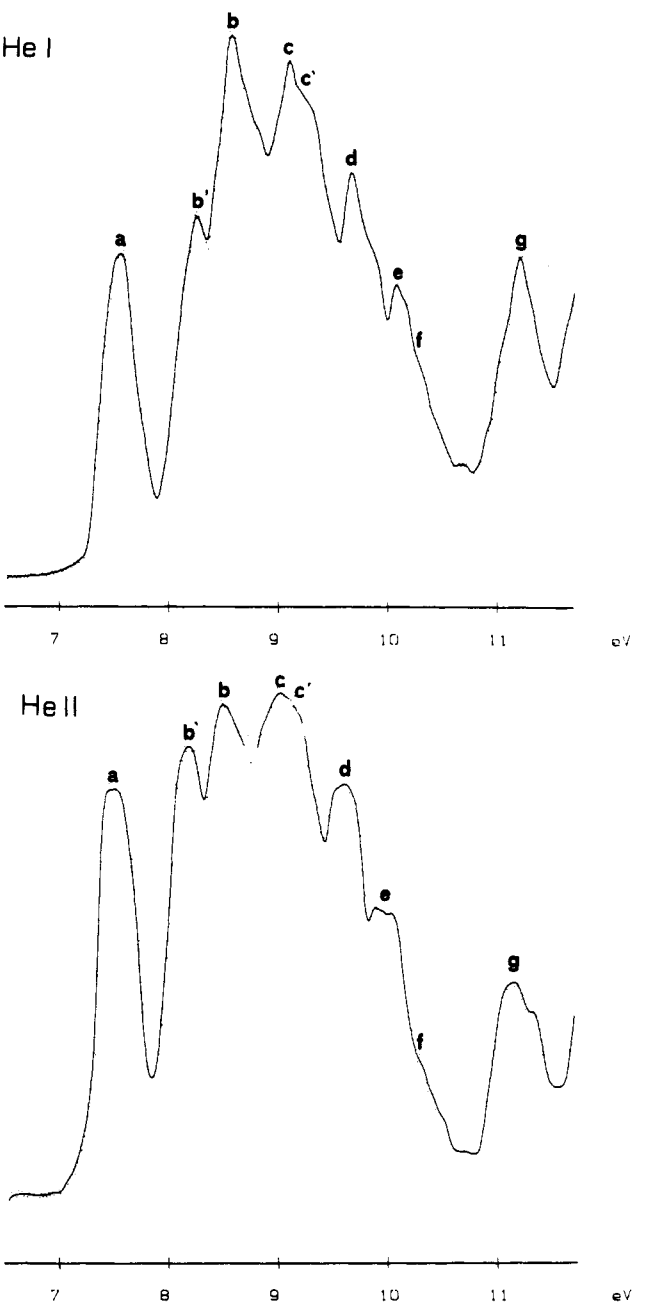

Figure 6. He I and He II photoelectron spectra of $Cp_2\overline{Zr}$-$(CH_2SiMe_2CH_2)$ (6.5–11.8-eV region).

the observed trend in orbital energies.[24c] The $15a_1$ LUMO (Figure 3), formerly $5a_1$ in the Cp_2Ti fragment, is slightly antibonding in character and is unoccupied. The overall result is a redistribution of electron density among the interacting fragments due to the ability of the $(\mu\text{-}CH_2)_2$ cluster to accept electron density from both the $>SiMe_2$ and Cp_2Ti fragments. Finally, note that charge is partly back-donated into the metallocene fragment. This mechanism helps restore the carbenoid character at the Ti center. The calculated metal charge, in fact (Table I), closely resembles that found in genuine Ti(II) complexes.[10a,25]

Similarities and differences observed for the remaining 1-sila-3-metallacyclobutanes can be accommodated within the same picture. In the Zr complex, due to the smaller metal–d admixture, the $9b_2$ MO is less stable but remains below the $14a_1$ (Table II). For the Mo complex, a slightly different orbital sequence is observed because of a nearly uniform 0.7-eV shift of π_2-related MOs (vide infra) (Table III). The HOMO $15a_1$ is predominantly a metal-based orbital with nearly equal contributions from the $4d_{x^2-y^2}$ and $4d_{z^2}$ orbitals, in accord with both the metal d^2 configuration and the conclusions of single-crystal EPR studies[26] performed on related paramagnetic d^1 Cp_2MX_2 complexes. In the model Th complex, the metal admixture into MOs formally representing the Th–C bonds ($14a_1$, $9b_2$) is smaller and has some 5f character, while the π_2-related MOs are admixed with both 5f and 6d metal AOs[12b] (Table IV;

(25) Rappé, A. K.; Goddard, W. A., III. *J. Am. Chem. Soc.* **1982**, *104*, 297–299.

(26) (a) Petersen, J. L.; Egan, J. W., Jr. *Inorg. Chem.* **1983**, *22*, 3571–3575. (b) Petersen, J. L.; Dahl, L. F. *J. Am. Chem. Soc.* **1975**, *97*, 6422–6433.

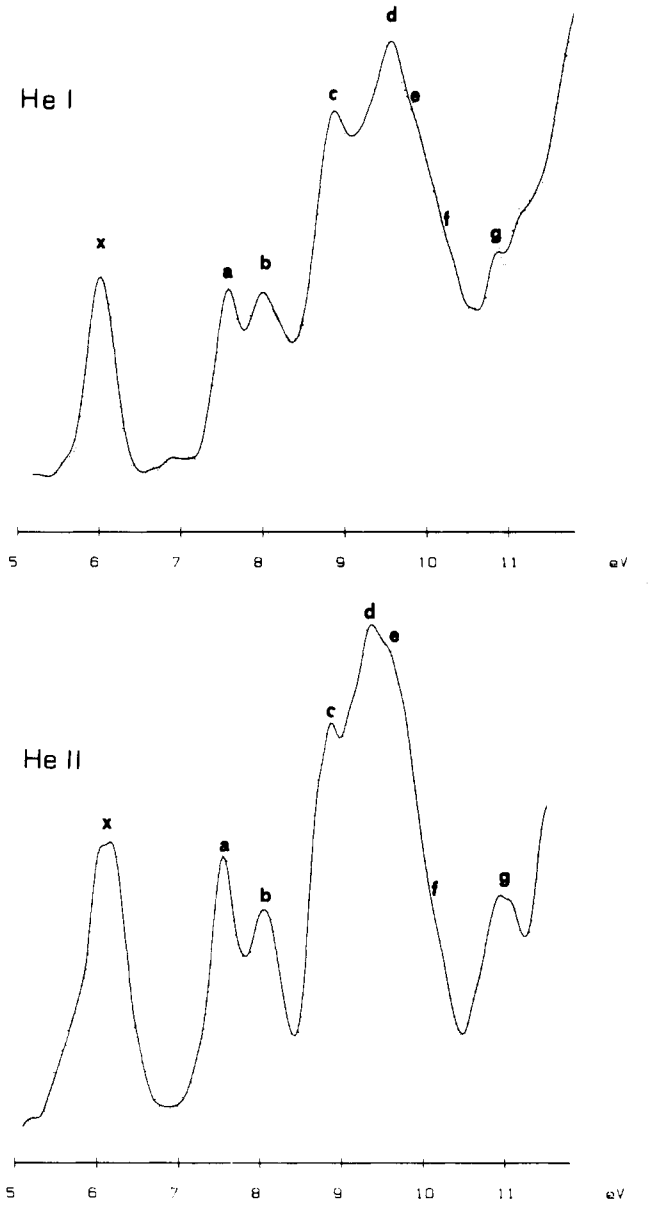

Figure 7. He I and He II photoelectron spectra of $Cp_2\overline{Mo(CH_2SiMe_2CH_2)}$ (5.0–11.8-eV region).

Figure 4). Finally, note that the energies of π_2-related MOs uniformly shift to higher values along the series Ti = Th < Zr < Mo. This observation agrees well with the trend of decreasing charges on the Cp rings (Tables I–IV).

Photoelectron Spectral Data. The gas-phase photoelectron spectroscopic data measured for $Cp_2\overline{M(CH_2SiMe_2CH_2)}$ (M = Ti, Zr, Mo) and $Cp'_2\overline{Th(CH_2SiMe_2CH_2)}$ complexes are entirely consistent with the calculated Xα TSIE results given in Tables I–IV, respectively. The PE spectra of $Cp_2Ti(\overline{CH_2SiMe_2CH_2})$ (Figure 5) contain nine bands in the region up to 11.5 eV, some of which are resolved only in the He II spectrum. The relative intensities of bands a and b increase to different extents in the He II spectrum.[27] On the basis of the Xα

(27) (a) Egdell, R. G.; Orchard, A. F. *J. Chem. Soc., Faraday Trans. 2* **1978**, *74*, 485–500. (b) Egdell, R. G.; Orchard, A. F. *J. Electron Spectrosc. Relat. Phenom.* **1978**, *14*, 277–286. (c) Egdell, R. G.; Orchard, A. F.; Lloyd, D. R.; Richardson, N. V. *J. Electron Spectrosc. Relat. Phenom.* **1977**, *12*, 415–423. (d) Egdell, R. C. Ph.D. Thesis, Oxford, 1979.

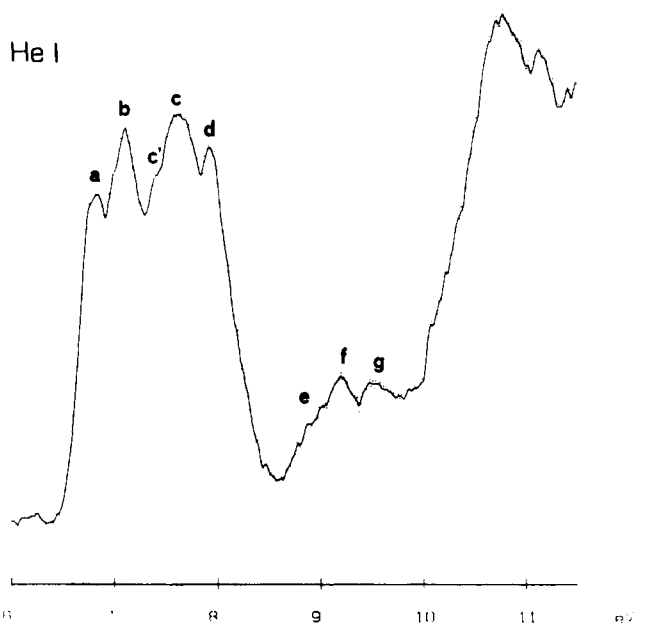

Figure 8. He I photoelectron spectrum of $Cp'_2\overline{Th(CH_2SiMe_2CH_2)}$ (6.0–11.8-eV region).

calculations (Table I), band a is assigned to ionization of the $14a_1$ HOMO. The small but significant increase in intensity in the He II spectrum reflects the relatively low metal 3d character (20%) of this MO.[27] The intensity of band b in the He I spectrum is about twice that of band a and, in accord with the calculations, represents the superposition of contributions from two ionization events associated with the $12b_1$ and $9b_2$ orbitals. Two distinct bands, b′ and b, are clearly resolved in He II spectrum. The more pronounced increase in intensity of component b is in accord with the greater metal $3d_{yz}$ character (32%) of the $9b_2$ Mo.[27] In contrast, the absence of any significant intensity enhancement for the b′ component in the He II spectrum is consistent with assignment to the π_2-Cp orbital, $12b_1$ (Table I). Bands c, c′, and d correspond to ionization of the three remaining π_2-Cp ring MOs ($7a_2$, $8b_2$, and $13a_1$). The relative intensities remain almost constant in the He II spectrum, consistent with a relatively low calculated metal–d content of these MOs. Finally, bands e, f, and g represent ionizations from more internal orbitals localized on the cyclobutane ring and on the $SiMe_2$ fragment (Table I).[23,28]

In both the He I and He II spectra of $Cp_2\overline{Zr(CH_2SiMe_2CH_2)}$, the profile of the b envelope is clearly resolved into distinct bands, b and b′ (Figure 6), with the intensity changes in the He II spectrum being opposite to the trend found in the Ti complex. In particular, the lower IE component b′ shows a much more pronounced increase than component b, consistent with the present Xα results which predict $9b_2$ to lie above the $12b_1$ level in the Zr complex (Table II). The remaining band assignments parallel those used earlier for the titanacycle (Table II).

The spectrum of $Cp_2\overline{Mo(CH_2SiMe_2CH_2)}$ shows one additional onset band (labeled x in Figure 7), which arises from the production of the ^2D ion state upon ionization of the $15a_1$ HOMO (Table III). As expected, the relative intensity of this band increases with He II radiation,

(28) Evans, S.; Green, J. C.; Joachim. P. J.; Orchard, A. F.; Turner, D. W.; Majer, J. P. *J. Chem. Soc., Faraday Trans. 2* **1972**, *68*, 905–911.

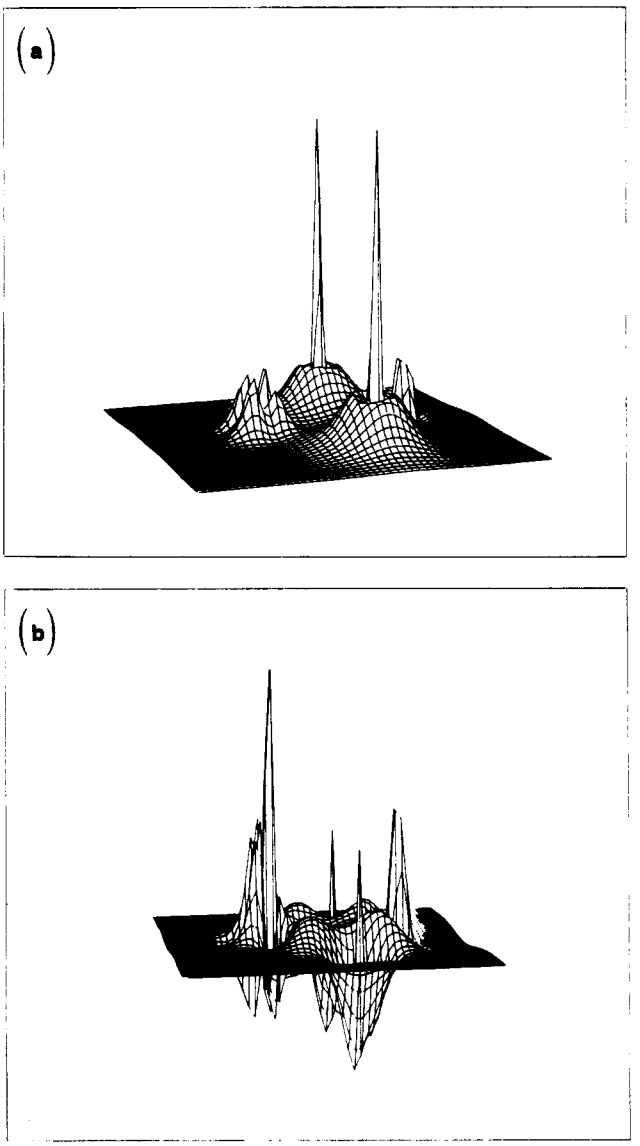

Figure 9. (a) Total charge density and (b) difference charge density pseudo-three-dimensional contour plots for the $Cp_2\overline{Ti(CH_2SiMe_2CH_2)}$ molecule in the *yz* plane.

consistent with the dominant metal 4d character of this MO.[27] Bands a and b clearly represent ionization from the $14a_1$ and $9b_2$ MOs. However, the greater enhancement of the intensity observed for band a compared to band b suggests the possibility of an inverted IE sequence with $9b_2 > 14a_1$. The remaining bands c, c', d, e, f, and g are assigned by comparison with theoretical Xα TSIE values, which are almost uniformly shifted by ca. 0.7 eV relative to their experimental IEs (Table III). The assignments convincingly fit both the observed band groupings and relative intensity changes in the He II spectrum (Figure 7).

The $Cp'_2\overline{Th(CH_2SiMe_2CH_2)}$ He I PE spectrum exhibits a different profile than encountered in the corresponding transition-metal complexes (Figure 8). This reflects both the expected IE shift to lower energies as a consequence of ring permethylation[15a,29] and the clustering of π_2 ionizations in a narrow energy range as anticipated by the

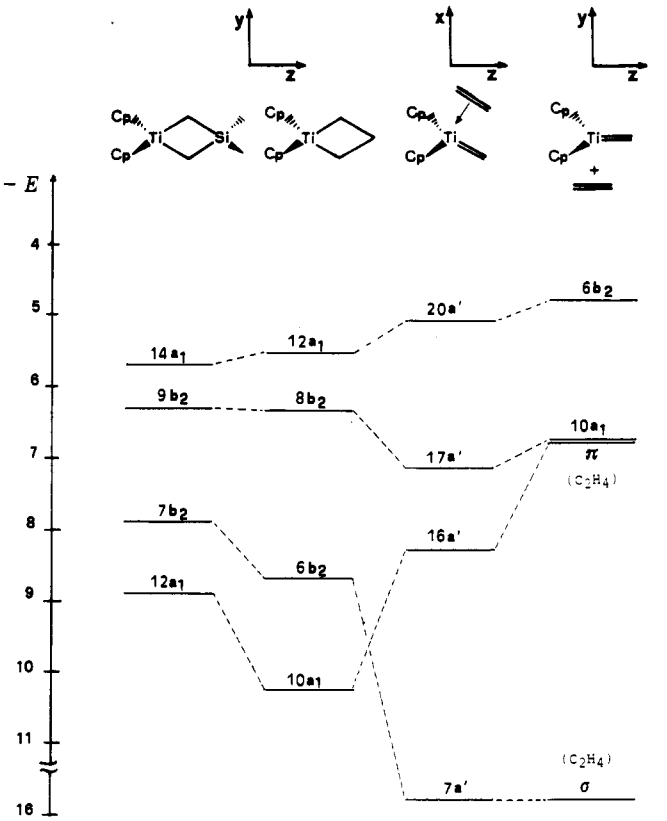

Figure 10. Evolution diagram of the relevant MOs of the 1-sila-3-titanacycle to an all-carbon titanacycle, to a titanamethylidene–olefin complex, to a titanamethylidene + olefin complex. Symmetry labels refer to the local coordinate systems shown above the structures.

calculations (Table IV). The spectrum is reminiscent of those of other Cp'_2ThX_2 (X = Cl, Me) complexes.[15a] Therefore, the assignment straightforwardly follows on the basis of both Xα TSIE results (Table IV) and simpler comparative arguments. The ionizations from Th–C (μ-CH_2) MOs are assigned to bands a and b. On the basis of relative intensity arguments, the more intense band b also represents the uppermost π_2-related MO ($12b_1$). Bands c and d are left for the remaining ionizations of π_2-related MOs (Table IV). The bands in the 8.5–10-eV region, are, finally, assigned to ionizations of MOs mostly localized on the $(\mu\text{-}CH_2)_2SiMe_2$ fragment (Table IV).

Discussion

The present results suggest that the electronic structures of 1-sila-3-metallacyclobutane complexes are better viewed electronically in terms of heterodinuclear species containing bridging μ-CH_2 groups rather than as simple hydrocarbyl derivatives. The formation of the four-membered ring involves bonding interactions analogous to those found in cyclobutane[24] and is characterized by an almost uniform accumulation of electron density in the internuclear regions of the metallacyclobutane ring. This is evident in total and difference charge density contour maps[30] (Figure 9). The metal–ligand bonding involves stabilizing interactions between higher-lying empty orbitals of the bridging μ-CH_2 groups and appropriate metal orbitals of

(29) Calabro, D. C.; Hubbard, J. L.; Belvins, C. H., II; Campbell, A. C.; Lichtenberger, D. L. *J. Am. Chem. Soc.* **1981**, *103*, 6839–6846.

(30) (a) Kutzler, F. W.; Sweptston, P. N.; Berkovitch-Yellin, Z.; Ellis, D. E.; Ibers, J. A. *J. Am. Chem. Soc.* **1983**, *105*, 2996–3004. (b) Delley, B.; Ellis, D. E. *J. Chem. Phys.* **1982**, *76*, 1949–1960. (c) Berkovitch-Yellin, Z.; Ellis, D. E. *J. Am. Chem. Soc.* **1981**, *103*, 6066–6073. (d) Ellis, D. E.; Berkovitch-Yellin, Z. *J. Chem. Phys.* **1981**, *74*, 2427–2435.

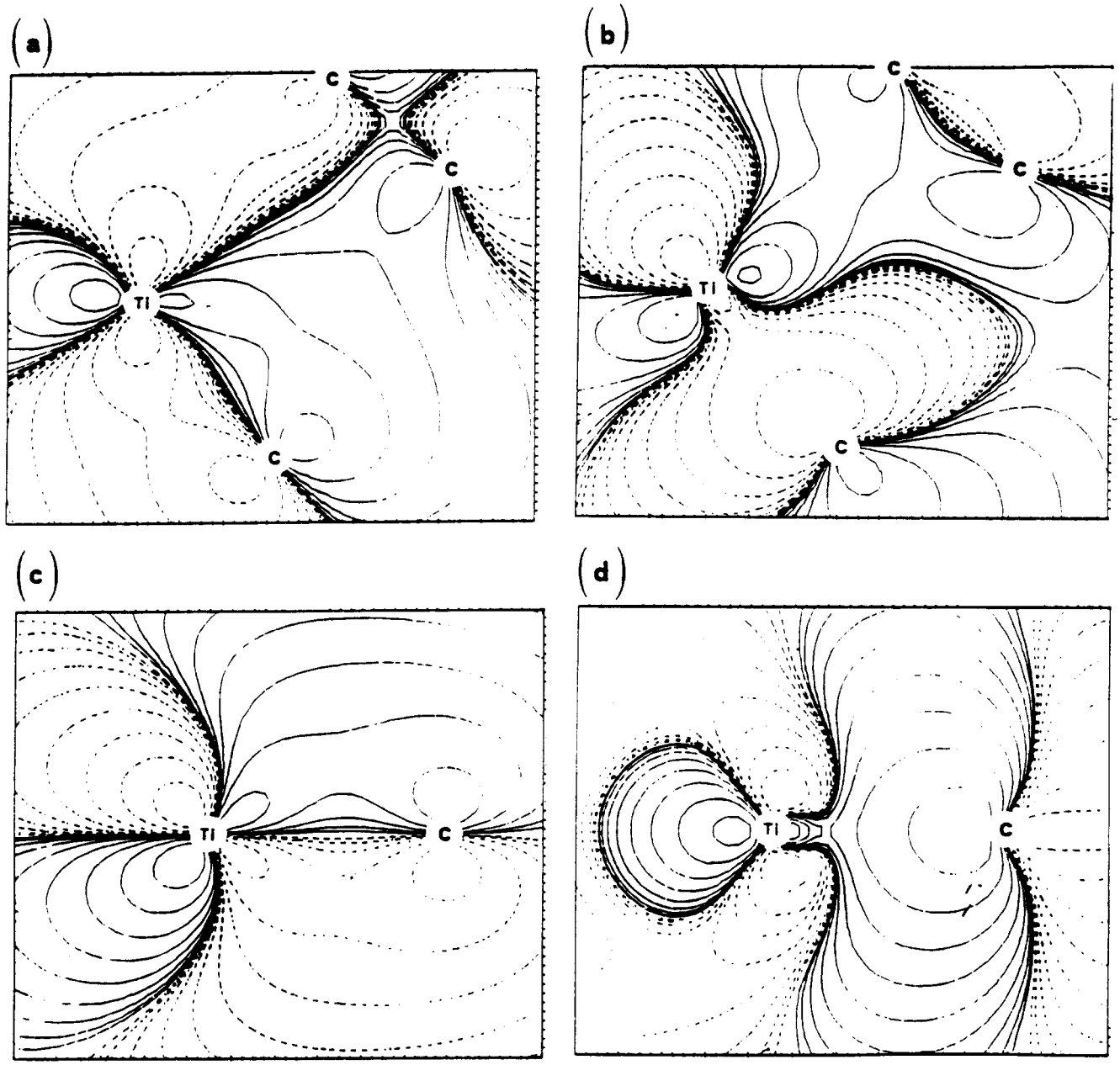

Figure 11. DV-Xα contour plots for the (a) 20a′ and (b) 17a′MOs of the $Cp_2Ti{=}CH_2(C_2H_4)$ molecule in the *xz* plane and for the (c) $6b_2$ and (d) $10a_1$ MOs of $Cp_2Ti{=}CH_2$ in the *yz* plane. The contour values are ±0.0065, ±0.013, ±0.026, ±0.052, ±0.104, ±0.208, ±0.416, and ±0.832 $e^{1/2}$ $Å^{3/2}$. Dashed lines refer to negative values.

the metallocene fragment. The resulting M–C bonds that accompany the stabilization of the "peripheral"[24] $14a_1$ and $9b_2$ orbitals, have energies modulated by the relative amounts of metal participation. The $7b_2$ and $12a_1$ "inner"[24] MOs provide, although to a lesser extent, some bonding contribution. The bonding interactions of the μ-CH_2 groups are reminiscent of those exhibited by classical ligands having both σ and π ligation capabilities[31] and help to rationalize why the Zr–C distance in $Cp_2\overline{Zr\text{-}(CH_2SiMe_2CH_2)}$[8c] is slightly shorter than in typical zirconocene bis(hydrocarbyl) complexes.[20a] The population of the aforementioned bonding orbitals permits donation of electron density primarily from the bridged $>SiMe_2$ fragment into the spatial region of the *yz* plane and is accompanied by metal-to-ligand back-donation of the carbenoid Cp_2Ti lone pair into the spatial region normal to the plane bisecting the C–M–C angle.

Many of the above points are also relevant to understanding the chemistry of these "stabilized" metallacyclobutanes and of the all-carbon metallacyclic compounds.[1-3] A distinctive reactivity mode[1-4] observed in titanacyclobutanes involves a metal–alkylidene intermediate, either as a simple methylidene complex or as an olefin–methylidene complex in thermal equilibrium with the metallacyclobutane (eq 1).[2b,d,e,17a] Although the activation energy[13] for this process is frequently low, theoretical evidence indicates that the metallacycle represents the thermodynamically-preferred structure for group 4.[13] The electronic alterations arising from metallacyclobutane–metallomethylidene–olefin complex interconversion are described well by the DV-Xα calculations on $Cp_2\overline{TiCH_2CH_2CH_2}$ (Table SV), on $Cp_2Ti{=}CH_2(C_2H_4)$

(31) Nugent, W. A.; Mayer, J. M. *Metal-Ligand Multiple Bonds*; Wiley Interscience: New York, 1988.

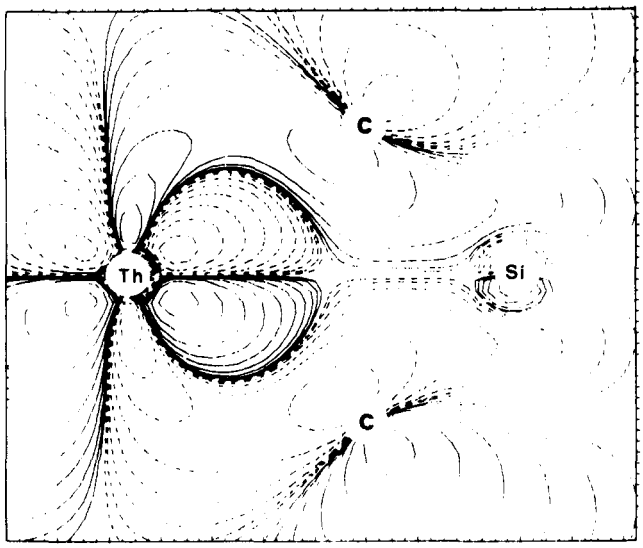

Figure 12. DV-Xα contour plot for the $10b_2$ MO of the $Cp_2\overline{Th(CH_2SiMe_2CH_2)}$ molecule in the yz plane. The contour values are ±0.0065, ±0.013, ±0.026, ±0.052, ±0.104, ±0.208, ±0.416, and ±0.832 $e^{1/2}$ Å$^{3/2}$. Dashed lines refer to negative values.

(Table V), and on noninteracting $Cp_2Ti{=}CH_2$ (Table SVI) + C_2H_4 molecules. It is noted that no major perturbations are found due to Si substitution at the β-position of the titanacyclobutane ring (Figure 10). The evolution of correlated MOs on traversing the aforementioned reaction coordinate reveals that the $12a_1$ and $8b_2$ MOs of the titanacyclobutane naturally evolve into the 20a′ and 17a′ MOs of the titanamethylidene–olefin complex, respectively (Figures 10 and 11). Their energy baricenter remains, however, approximately constant. In contrast, the 16a′ and 7a′ MOs of the alkylidene–olefin complex, which are almost identical to those of the free olefin,[13] are modified in the $2_\pi + 2_\pi$ cycloaddition[13] process which generates the metallacycle. Nevertheless, the contribution of these MOs to the metal–ligand bonding is small[13] and, hence, the contribution to the overall stability of the metallacycle is similarly small. The titanacycle ($Cp_2\overline{TiCH_2CH_2CH_2}$) can be considered as a latent olefin complex[2d] even though the metallacyclic structures is thermodynamically preferred. The relative importance of the metal–methylidene structure in the reactivity displayed by other metallacyclobutane complexes, however, has been shown to be influenced by the capacity of the metal to form covalent bonds.[25,32] *Therefore, the present finding of decreasing metal–d covalency (Tables I, II, and IV) with Ti ≥ Zr ≫ Th parallels the tendency to traverse the reaction coordinate of eq 1.* Likewise, the greater protonolytic reactivity of Th–alkyl bonds vis-à-vis Zr–alkyl bonds[6,20a] accords with the present findings about covalency. In general, the chemistry displayed by group 4 metallacyclobutanes is largely orbitally controlled. For the d^0 Ti and Zr complexes, the LUMO ($15a_1$) is M–C antibonding and is primarily d_{z^2}, $d_{x^2-y^2}$ in character. Its spatial orientation (Figure 3) favors a lateral approach along the y axis (Chart I) by an incoming substrate. Subsequent electron donation into this orbital weakens the adjacent M–C bond, thereby either inducing insertion of the substrate into the M–C bond, as observed for $(C_5R_5)_2\overline{Zr(CH_2SiMe_2CH_2)}$ (R = H, Me),[33] or the displacement of an olefin from $Cp_2\overline{Ti(CH_2CR^1R^2CH_2)}$.[2b,d] In the corresponding Mo complex, the population of the $15a_1$ orbital by the d^2 lone pair should instead favor electrophilic attack at the metal center (as observed).[26,34] Finally, in the Th complex the LUMO ($10b_2$ in Figure 12) is nonbonding with some 5f character. The substantially lower metal d character observed here suggests that substrate insertion[6a] into the Th–C bonds of $Cp'_2\overline{Th(CH_2SiMe_2CH_2)}$ is probably not orbitally controlled but rather governed by a combination of charge effects[17b,35] and a strong propensity to reduce the ring strain.[36]

Chart I

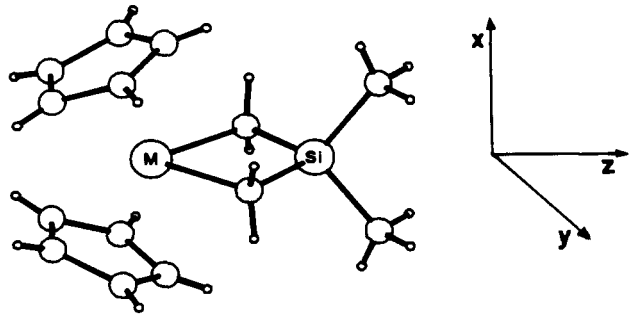

Acknowledgment. We gratefully thank the Ministero della Pubblica Istruzione "MPI, ROMA, ITALY" (E.C., I.F.), the Petroleum Research Fund, as administered by the American Chemical Society (J.L.P.), and the National Science Foundation (T.J.M., Grant CHE 9104112) for financial support.

Registry No. $Cp_2\overline{Ti(CH_2Si(CH_3)_2CH_2)}$, 71515-00-9; $Cp_2\overline{Zr(CH_2Si(CH_3)_2CH_2)}$, 89530-31-4; $Cp_2\overline{Mo(CH_2Si(CH_3)_2CH_2)}$, 89530-33-6; $Cp_2\overline{Th(CH_2Si(CH_3)_2CH_2)}$, 89302-73-8; $Cp_2Ti{=}CH_2(C_2H_4)$, 79105-33-2.

Supplementary Material Available: Tables SI, SII, SIII, and SIV of unoccupied orbitals, eigenvalues, and population analyses for $Cp_2\overline{Ti(CH_2SiMe_2CH_2)}$, $Cp_2\overline{Zr(CH_2SiMe_2CH_2)}$, $Cp_2\overline{Mo(CH_2SiMe_2CH_2)}$, and $Cp_2\overline{Th(CH_2SiMe_2CH_2)}$, respectively, and Tables SV and SVI of orbitals, eigenvalues, and population analysis of $Cp_2\overline{TiCH_2CMe_2CH_2}$ and $Cp_2Ti{=}CH_2$, respectively (6 pages). Ordering information is given on any current masthead page.

(32) (a) Carter, E. A.; Goddard, W. A., III. *J. Am. Chem. Soc.* **1986**, *108*, 4746–4754. (b) Gregory, A. R.; Mintz, E. A. *J. Am. Chem. Soc.* **1985**, *107*, 2179–2180. (c) Eisenstein, O.; Hoffmann, R.; Rossi, A. R. *J. Am. Chem. Soc.* **1981**, *103*, 5582–5584.

(33) (a) Berg, F. J.; Petersen, J. L. *Organometallics* **1989**, *8*, 2461–2470. (b) Petersen, J. L.; Egan, J. W., Jr. *Organometallics* **1987**, *6*, 2007–2008. (c) Tikkanen, W. R.; Petersen, J. L. *Organometallics* **1984**, *3*, 1651–1655.

(34) Anslyn, E. V.; Goddard, W. A., III. *Organometallics* **1989**, *8*, 1550–1558.

(35) The Xα charge found on the Th metal center is +2.18 (Table IV).

(36) Bruno, J. W.; Marks, T. J.; Morss, L. J. *J. Am. Chem. Soc.* **1983**, *105*, 6824–6832.